X-ray Absorption Studies of Three-Coordinate Dicopper(I) Complexes and Their Dioxygen Adducts

Ninian J. Blackburn,*[1a,c] Richard W. Strange,[1a] Amjad Farooq,[1b] Michael S. Haka,[1b] and Kenneth D. Karlin*[1b]

Contribution from the Department of Chemistry, University of Manchester Institute of Science and Technology, P.O. Box 88, Manchester M60 1QD, U.K., and Department of Chemistry, State University of New York, Albany, New York 12222. *Received July 13, 1987*

Abstract: Recently, the preparation and preliminary characterization of a new series of dioxygen complexes derived from the ligand systems N4PY2, N3PY2, and N3ORPY2 have been reported. These compounds, $[Cu_2L(O_2)]^{2+}$ (**4-6**), are derived from well-characterized dicopper(I) complexes, $[Cu_2L]^{2+}$ (**1-3**), by the reversible reaction with dioxygen in dichloromethane at -80 °C (Cu:O_2 = 2:1). X-ray absorption spectra of the dioxygen adducts (**4-6**), their dicopper(I) precursors (**1-3**), and other related pyridyl ligand containing Cu(I) and Cu(II) complexes are reported. The results of edge and EXAFS analysis support a description of the oxygen adducts as four- or five-coordinated peroxo-bridged dicopper(II) complexes, with Cu-Cu distances in the range 3.2-3.4 Å. Possible structures for $[Cu_2(L)(O_2)]^{2+}$ are proposed including a novel $\eta^2:\eta^2$ peroxo coordination mode. In addition, the detailed analyses of the crystallographically characterized Cu(I) precursor complexes and related Cu(II) complexes of known structure have extended to pyridyl-containing systems the validity of the multiple scattering method of EXAFS analysis (the success of which has been demonstrated recently for imidazole-containing complexes and protein derivatives).

The binding and activation of dioxygen by active-site metal ions is central to the understanding of the mechanism of copper oxidase and oxygenase enzymes. Extensive spectroscopic studies on the O_2-carrying protein hemocyanin (Hc)[2-5] have provided a detailed description of the oxygen binding site and support a structure for oxy-Hc comprised of two tetragonal Cu(II) centers, each coordinated to two or three histidine ligands and bridged by an exogenous protein ligand. Resonance Raman,[2] optical,[3] and CD[3] studies indicate that the O_2 is coordinated as a 1,2-μ-peroxo moiety, bridging a pair of strongly antiferromagnetically coupled Cu(II) ions.[5] A Cu-Cu distance of 3.6 ± 0.1 Å has been determined for oxy-Hc by EXAFS spectroscopy, but there is disagreement in the literature concerning the presence or absence of an EXAFS-detectable Cu-Cu interaction in the deoxy form.[4]

The recent X-ray crystal structure of *Panulirus interruptus* deoxyhemocyanin[6] has confirmed many features of the spectroscopic model of the dioxygen binding site. Each copper of the dinuclear unit is coordinated to three histidines via the nitrogen atoms of the imidazole groups. The Cu-Cu distance is determined as 3.8 ± 0.4 Å. However, the presence of a protein-derived endogenous bridge (e.g., tyrosine or serine) is not supported by the X-ray data nor is any such residue located within a radius of ca. 17 Å of the copper site in deoxy-Hc. Thus, if there is a bridging ligand other than peroxide, hydroxide or water seems the most likely candidate.

Dioxygen binding to copper is also of interest because of its putative role in the mechanism of monooxygenase enzymes such as tyrosinase and dopamine-hydroxylase. No X-ray data are presently available for any copper oxidase or oxygenase enzyme, but an oxygen complex of tyrosinase (which catalyzes monophenol hydroxylation) has been isolated and studied spectroscopically.[7,11a] On the basis of both spectroscopic comparisons[8] and sequence homologies,[9] it is clear that an analogous dinuclear oxygen binding site is present in tyrosinase, with a reported Cu-Cu distance of 3.63 Å.[10] The monooxygenase activity of the enzyme has been attributed to more facile access of substrates to the active site.[11]

In contrast, no evidence exists for dinuclear copper at the active site of dopamine-hydroxylase (which catalyzes the benzylic hydroxylation of ring-substituted phenylethylamines),[12,13] although two coppers per subunit have been implicated in the mechanism[14] with an enzyme-bound hydroperoxide entity proposed as an intermediate.[15] A rich and varied chemistry thus exists for the activation and reaction of dioxygen at enzyme-bound copper centers, which is still incompletely understood.

Structural studies on relevant biomimetic models offer a powerful adjunct to structural and spectroscopic studies on the enzymes themselves and help to elucidate the important structural, electronic, and mechanistic factors that control catalysis.[16] The chemistry of a reversibly bound dioxygen adduct of a phenolato-bridged dicopper(I) complex, $[Cu_2(XYL\text{-}O\text{-})O_2]^+$ is now well developed,[17-19] and detailed characterization of this metastable

(1) (a) University of Manchester Institute of Science and Technology. (b) SUNY, Albany. (c) Present address: Department of Chemical and Biological Sciences, Oregon Graduate Center, Beaverton, OR 97006.

(2) Freedman, T. B.; Loehr, J. S.; Loehr, T. M. *J. Am. Chem. Soc.* **1976**, *92*, 2809-2815.

(3) (a) Eickman, N. C.; Himmelwright, R. S.; Solomon, E. I. *Proc. Natl. Acad. Sci. U.S.A.* **1979**, *76*, 2094-2098. (b) Himmelwright, R. S.; Eickman, N. C.; Solomon, E. I. *J. Am. Chem. Soc.* **1979**, *101*, 1576-1586. (c) Himmelwright, R. S.; Eickman, N. C.; LuBien, C. D.; Solomon, E. I. *J. Am. Chem. Soc.* **1980**, *102*, 5378-5388. (d) Wilcox, D. E.; Long, J. R.; Solomon, E. I. *J. Am. Chem. Soc.* **1984**, *106*, 2186-2194.

(4) (a) Co, M. S.; Hodgson, K. O. *J. Am. Chem. Soc.* **1981**, *103*, 984-986. (b) Co, M. S.; Hodgson, K. O. *J. Am. Chem. Soc.* **1981**, *103*, 3200-3201. (c) Brown, J. M.; Powers, L.; Kincaid, B.; Larrabee, J. A.; Spiro, T. G. *J. Am. Chem. Soc.* **1980**, *102*, 4210-4216. (d) Woolery, G. L.; Powers, L.; Winkler, M.; Solomon, E. I.; Spiro, T. G. *J. Am. Chem. Soc.* **1984**, *106*, 86-92.

(5) Moss, T. H.; Gould, D. C.; Ehrenberg, A.; Loehr, J. S.; Mason, H. S. *Biochemistry* **1973**, *12*, 2444-2449.

(6) Gaykema, W. P. J.; Volbeda, A.; Hol, W. G. J. *J. Mol. Biol.* **1985**, *187*, 255-275.

(7) Jolley, R. L.; Evans, L. H.; Makino, N.; Mason, H. S. *J. Biol. Chem.* **1974**, *249*, 335-345.

(8) Himmelwright, R. S.; Eickman, N. C.; LuBien, C. D.; Lerch, K.; Solomon, E. I. *J. Am. Chem. Soc.* **1980**, *102*, 7339-7344.

(9) Lerch, K.; Huber, M.; Schneider, H. J.; Drexel, R.; Bernt, L. *J. Inorg. Biochem.* **1986**, *26*, 213-217.

(10) Woolery, G. L.; Powers, L.; Winkler, M.; Solomon, E. I.; Lerch, K.; Spiro, T. G. *Biochim. Biophys. Acta* **1984**, *788*, 155-161.

(11) (a) Winkler, M. E.; Lerch, K.; Solomon, E. I. *J. Am. Chem. Soc.* **1981**, *103*, 7001-7003. (b) Wilcox, D. E.; Porras, A. G.; Hwang, Y. T.; Lerch, K.; Winkler, M. E.; Solomon, E. I. *J. Am. Chem. Soc.* **1985**, *107*, 4015-4027.

(12) (a) Lerch, K. *Met. Ions Biol. Syst.* **1981**, *13*, 143-186. (b) Villafranca, J. J. *Met. Ions Biol. 3*, 263-290.

(13) (a) Blackburn, N. J.; Collison, D.; Sutton, J.; Mabbs, F. E. *Biochem. J.* **1984**, *220*, 447-454. (b) Ljones, T.; Flatmark, T.; Skotland, T.; Petersson, L.; Backstrom, D.; Ehrenberg, A. *FEBS Lett.* **1978**, *92*, 81-84. (c) Walker, O. A.; Kon, H.; Lovenberg, W. *Biochim. Biophys. Acta* **1977**, *482*, 309-322.

(14) (a) Klinman, J. P.; Krueger, M.; Brenner, M.; Edmondson, D. E. *J. Biol. Chem.* **1984**, *259*, 3399-3402. (b) Ash, D. E.; Papadopoulos, N. J.; Colombo, G.; Villafranca, J. J. *J. Biol. Chem.* **1984**, *259*, 3395-3398. (c) Blackburn, N. J.; Mason, H. S.; Knowles, P. F. *Biochem. Biophys. Res. Commun.* **1980**, *95*, 1275-1282.

(15) Miller, S. M.; Klinman, J. P. *Biochemistry* **1985**, *24*, 2114-2127.

(16) (a) Karlin, K. D., Zubieta, J., Eds. *Biological and Inorganic Copper Chemistry*; Adenine: Guilderland, NY, 1986; Vol. 1 and 2. (b) Karlin, K. D.; Gultneh, Y. *J. Chem. Educ.* **1985**, *62*, 983-990. (c) Karlin, K. D.; Gultneh, Y. *Prog. Inorg. Chem.* **1987**, *35*, 219-327.

0002-7863/88/1510-4263$01.50/0

Scheme I. Description of the Ligand Systems, Their Cu(I) and Cu(II) Complexes, and the Adducts with O_2

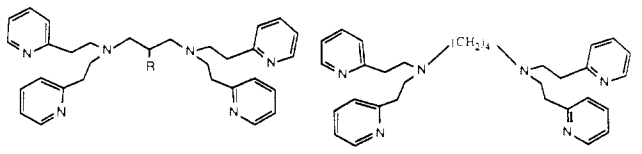

R = H N3PY2 N4PY2

R = $OC(O)C_6H_4$-C_6H_5 N3ORPY2

$[Cu_2(N3PY2)(CH_3CN)_2][ClO_4]_2$: 1

$[Cu_2(N3ORPY2)][PF_6]_2$: 2

$[Cu_2(N4PY2)(CH_3CN)_2][ClO_4]_2$: 3

$[Cu_2(N4PY2)][ClO_4]_2$: 3

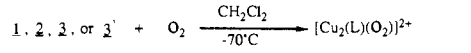

L = N3PY2 : 4

L = N3ORPY2 : 5

L = N4PY2 : 6

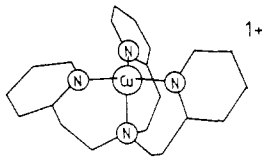

7

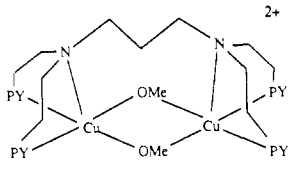

8

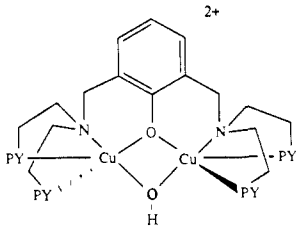

9

dicopper(II)–peroxo complex has been achieved using UV–vis,[17b] resonance Raman,[18] and EXAFS[19] spectroscopies. Recently the preparation and preliminary characterization of a new series of dioxygen complexes derived from the ligand systems N4PY2, N3PY2, and N3ORPY2 (Scheme I) were reported. These compounds, $[Cu_2L(O_2)]^{2+}$ (**4–6**), are derived from well-characterized dicopper(I) complexes, $[Cu_2L]^{2+}$ (**1–3**), by the reversible reaction with dioxygen in dichloromethane at −80 °C (Cu:O_2 = 2:1);[20] the UV–vis spectral properties of **4–6** bear a close resemblance to those of oxy-Hc.[20,21] The ligands differ from the analogous (XYL-O-) system in that no "endogenous" donor ligand is present. They therefore act as useful models for the spectroscopic evaluation of purely exogenous bridged structures. Like $[Cu_2(XYL\text{-}O\text{-})O_2]^+$, these oxy complexes are only stable below −50 °C and crystallographic characterization has not yet proved possible. We have therefore resorted to spectroscopic characterization and report here details of an X-ray absorption study of the dioxygen adducts, their dicopper(I) precursors, and other related pyridyl ligand containing Cu(I) and Cu(II) complexes. The results support a description of the oxygen adducts as four- or five-coordinated peroxo-bridged dicopper(II) complexes, with Cu–Cu distances in the range 3.2–3.4 Å.

Materials and Methods

Syntheses of Ligands, Complexes, and Their Acetonitrile Adducts. Details of the synthesis of the ligands N3PY2, N3ORPY2, and N4PY2, their dicopper(I) complexes (**1–3** and **3′**), and dioxygen adducts (**4–6**) are provided elsewhere.[20–22]

Preparation of Samples for EXAFS Measurements. The oxygenated complexes **4–6** were prepared and transferred to the EXAFS cell in a single operation as follows. Portions (0.03–0.05 g) of the acetonitrile derivative of the dicopper(I) dication as either hexafluorophosphate (**2**) or perchlorate (**1**, **3**, **3′**) were dissolved in 1.5 cm^3 of deoxygenated dichloromethane (redistilled over P_2O_5), in a small tube with a side arm connected to the EXAFS cell via 0.2-mm-thick capillary tubing. The resultant pale yellow solutions were cooled to −78 °C by immersing the flask, tubing, and EXAFS cell in solid powdered dry ice. When the solution was cold, a stream of pure oxygen was admitted via a stopcock connected to the side arm. The solution immediately darkened to deep magenta (**4**) or brown (**5**, **6**) as described previously.[20] The oxygenated solution was then transferred to the EXAFS cell by application of a slight positive pressure to the apparatus. The cells were then rapidly frozen in liquid nitrogen and stored under liquid N_2 until use (typically 2–5 days). In one experiment involving the N4PY2 ligand system, the three-coordinate $[Cu_2L](ClO_4)_2$ complex (**3′**) rather than the four-coordinate acetonitrile adduct (**3**) was used. This gave an identical EXAFS spectrum. Identical spectra were also recorded for samples of all the complexes stored in liquid nitrogen for a period of 4 weeks, indicating that no measurable deterioration was occurring during storage at 77 K.

EXAFS Data Collection and Analysis. Aluminum cells with rectangular apertures (12 × 3 mm) and a sample thickness of 2 mm were used. The frozen solutions of the oxygenated complexes were measured in fluorescence mode,[23] while the dicopper(I), Cu^ITEPA, and dicopper(II) model complexes were measured as powders in transmission mode, using stations 7.1, 8.2, and 9.2 at the SRS, Daresbury Laboratory, under operating conditions of 2.00 GeV and maximum currents of 300 mA. The temperature was maintained at 12–20 K by an Oxford Instruments continuous-flow helium cryostat, specially designed for the EXAFS experiments. Si(220) or Si(111) double-crystal order sorting monochromators were used with harmonic rejection, typically chosen to be 50%. In each case, the monochromator was calibrated in energy space by setting the maximum of the first feature on the absorption edge of metallic copper foil to 8982 eV, measured under identical conditions.

Six scans were taken for each oxygenated sample, which were later averaged, while a single scan was sufficient for powdered model compounds. Established procedures[24,25] were used to extract the EXAFS oscillations from absorption or fluorescence data. After conversion of monochromator position to energy and normalization of the edge height, background subtraction was achieved by fitting the smoothly varying part of the absorption to polynomials below and above the absorption edge and subtracting from the experimental absorption spectrum. The background-subtracted, raw EXAFS thus obtained was converted into *k* space

(17) (a) Karlin, K. D.; Cruse, R. W.; Gultneh, Y.; Hayes, J. C.; Zubieta, J. *J. Am. Chem. Soc.* **1984**, *106*, 3372–3374. (b) Karlin, K. D.; Cruse, R. W.; Gultneh, Y.; Farooq, A.; Hayes, J. C.; Zubieta, J. *J. Am. Chem. Soc.* **1987**, *109*, 2668–2679.

(18) Pate, J. E.; Cruse, R. W.; Karlin, K. D.; Solomon, E. I. *J. Am. Chem. Soc.* **1987**, *109*, 2624–2630.

(19) Blackburn, N. J.; Strange, R. W.; Cruse, R. W.; Karlin, K. D. *J. Am. Chem. Soc.* **1987**, *109*, 1235–1237.

(20) (a) Karlin, K. D.; Haka, M. S.; Cruse, R. W.; Gultneh, Y. *J. Am. Chem. Soc.* **1985**, *107*, 5828–5829. (b) Karlin, K. D.; Haka, M. S.; Cruse, R. W.; Meyer, G. J.; Farooq, A.; Gultneh, Y.; Hayes, J. C.; Zubieta, J. *J. Am. Chem. Soc.* **1988**, *110*, 1196–1207.

(21) Farooq, A. Ph.D. Dissertation, State University of New York at Albany, 1987.

(22) Haka, M. S. Ph.D. Dissertation, State University of New York at Albany, 1987.

(23) Hasnain, S. S.; Quinn, P. D.; Diakun, G. P.; Wardell, E. M.; Garner, C. D. *J. Phys. E* **1984**, *17*, 40–43.

(24) (a) Teo, B. K. In *EXAFS Spectroscopy: Techniques and Applications*; Teo, B. K., Joy, D. C., Eds.; Plenum: New York, 1981; pp 13–58. (b) Cramer, S. P.; Hodgson, K. O. *Prog. Inorg. Chem.* **1979**, *25*, 1–39.

(25) Strange, R. W.; Blackburn, N. J.; Knowles, P. F.; Hasnain, S. S. *J. Am. Chem. Soc.* **1988**, *109*, 7157–7162.

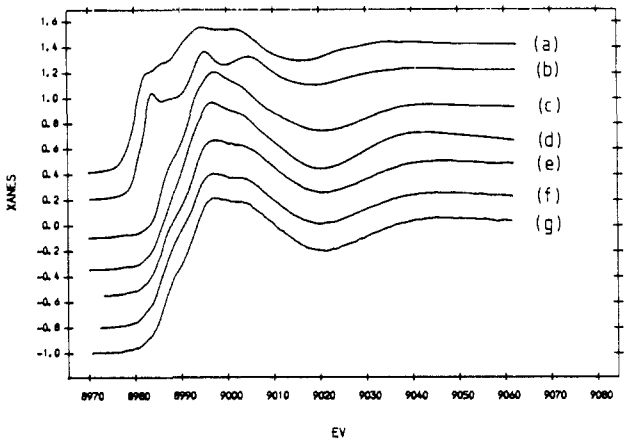

Figure 1. Cu K absorption edges for (a) complex **3'**, (b) complex **2**, (c) complex **8**, (d) the azido adduct of complex **9**,[36b] (e) oxygenated complex **5**, (f) oxygenated complex **6**, and (g) oxygenated complex **4**.

and weighted, usually by k^3, in order to compensate for the diminishing amplitude at high k due to decay of the photoelectron wave. Analysis of the EXAFS was carried out by the nonlinear least-squares program EXCURVE[26] as previously described.[25-29] An ab initio approach was used to calculate the atomic phase shifts as described in ref 25 and 26. Multiple scattering calculations were carried out as described in references 25, 26, 28, and 29. The goodness of fit was judged both qualitatively and quantitatively with use of a goodness-of-fit parameter, or "fit index" (FI), defined as

$$\mathrm{FI} = \sum_i [X(i)_{\mathrm{exptl}} - X(i)_{\mathrm{theory}}]^2 / N$$

where N is the number of data points in the experimental spectrum.

Results and Discussion

Absorption Edges and Near-Edge Structure (XANES). Figure 1 shows the Cu K absorption edges of the oxygenated compounds **4–6**, together with those of the dicopper(I) precursor complexes **2** and **3**, and the two related dicopper(II) compounds **8** and **9** (Scheme I). The prominent edge feature present in the Cu(I) compounds is not observed in the oxygenated complexes, and the edge position has shifted from 8983 to 8987 eV. The absorption edges of **4–6** resemble closely those of the dicopper(II) compounds **8** and **9** both in energy and in the shape and position of the poorly resolved features occurring at 8986, 8995, 8998, and 9004 (±1) eV. These similarities in edge structure imply that the inter- and intraligand multiple scattering interactions giving rise to the XANES features[33] are very similar in the oxygenated complexes and the dicopper(II) models and thus suggest structural similarities. It is possible on the basis of these edge comparisons to assign with confidence an oxidation state of +2 to the oxygenated complexes **4–6**. The 2:1 Cu to O_2 stoichiometry observed for dioxygen uptake[20-22] would then require the oxygen to be bound as peroxide, similar to the situation in the related $[Cu_2(XLY\text{-}O\text{-})(O_2)]^+$ complex described previously.[17b-19]

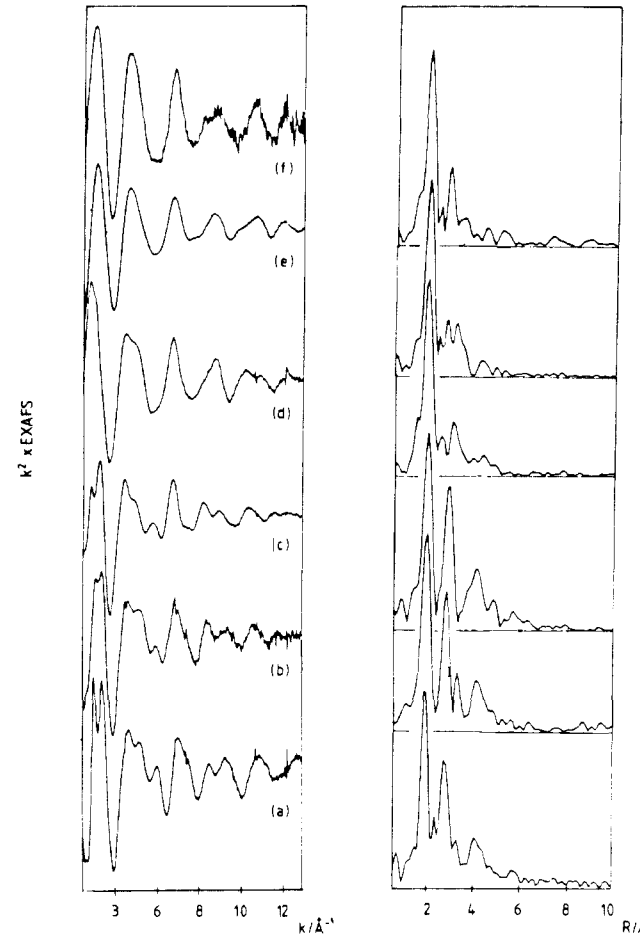

Figure 2. k^2-Weighted experimental Cu K EXAFS and Fourier transforms for (a) complex **2**, (b) complex **3'**, (c) complex **7**, (d) complex **8**, (e) complex **9**, and (f) oxygenated complex **6**.

Table I. Atom-Labeling Scheme for Pyridine Groups, Pathways, and Expected Angles for Double and Triple Scattering Interactions in Cu–Pyridine Complexes

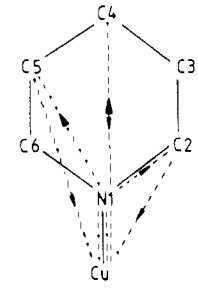

pathway	angle/deg	pathway	angle/deg
Cu–N1–C2	+120	Cu–N1–C5	−150
Cu–N1–C2	−120	Cu–N1–C4	180
Cu–N1–C3	+150		

Extended X-ray Absorption Fine Structure (EXAFS). Figure 2 shows the k^2-weighted Cu K edge EXAFS and Fourier transforms of the oxy complex **6** (Figure 2f), compared with those of the dicopper(I) precursors **2** and **3'** (Figure 2a,b), and it is clear that significant differences exist between the spectra of the oxy complex and its precursor. The Cu(I) complexes contain an intense first-shell peak in the Fourier transform at ca. 2.0 Å and additional strong peaks at ca. 3.0 and 4–5 Å. However, the

(26) (a) Gurman, S. J.; Binsted, N.; Ross, I. *J. Phys. C* **1984**, *17*, 143–151. (b) Gurman, S. J.; Binsted, N.; Ross, I. *J. Phys. C* **1986**, *19*, 1845–1861. (c) Lee, P. A.; Pendry, J. B. *Phys. Rev. B* **1975**, *11*, 2795–2811.

(27) (a) Blackburn, N. J.; Hasnain, S. S.; Binsted, N.; Diakun, G. P.; Garner, C. D.; Knowles, P. F. *Biochem. J.* **1984**, *219*, 985–990. (b) Blackburn, N. J.; Hasnain, S. S. In *Biological and Inorganic Copper Chemistry*; Karlin, K. D., Zubieta, J., Eds.; Adenine: Guilderland, NY, 1986; Vol. II, pp 33–42.

(28) Blackburn, N. J.; Strange, R. W.; McFadden, L.; Hasnain, S. S. *J. Am. Chem. Soc.* **1988**, *109*, 7162–7170.

(29) The angular dependence of the forward scattering and the contribution of multiple scattering to the total EXAFS are summarized in eq 2.1 and 3.1 of ref 26c. The forward scattering, which is energy dependent, peaks strongly at angles of $n\pi$ (n = 0, 1, 2, ...) as shown in Figure 5 of ref 26c.

(30) Karlin, K. D.; Shi, J.; Hayes, J. C.; McKown, J. W.; Hutchinson, J. P.; Zubieta, J. *Inorg. Chim. Acta* **1984**, *91*, L3–L7.

(31) Karlin, K. D.; Hayes, J. C.; Gultneh, Y.; Cruse, R. W.; McKown, J. W.; Hutchinson, J. P.; Zubieta, J. *J. Am. Chem. Soc.* **1984**, *106*, 2121–2128.

(32) (a) Karlin, K. D.; Hayes, J. C.; Hutchinson, J. P.; Hyde, J. R.; Zubieta, J. *Inorg. Chim. Acta* **1982**, *64*, L219. (b) Zubieta, J.; Karlin, K. D.; Hayes, J. C. *Copper Coordination Chemistry: Biochemical and Inorganic Perspectives*; Karlin, K. D., Zubieta, J., Eds.; 1983; pp 97–108.

(33) (a) Smith, T. A.; Penner-Hahn, J. E.; Berding, M. A.; Doniach, S.; Hodgson, K. O. *J. Am. Chem. Soc.* **1985**, *107*, 5945–5955. (b) Durham, P. J.; Pendry, J. B.; Hodges, C. H. *Comput. Phys. Commun.* **1982**, *25*, 193.

outer-shell peaks of the oxygenated complex are much less intense relative to the intensity of the first-shell peak. Interpretation of such differences will clearly be important in the structural characterization of the oxygenated species.

The pattern of outer-shell transform peaks exhibited by the dicopper(I) complexes is similar to that observed in the EXAFS of metal complexes containing imidazole ligation, which is known to arise from scattering from first-shell nitrogen atoms (ca. 2 Å), C2/C5 carbon atoms (ca. 3 Å), and C3/N4 carbon and nitrogen atoms (ca. 4 Å) of the rigid planar imidazole ring.[25,27,28] We have recently shown[25,28] that both single and multiple scattering interactions are necessary to describe the EXAFS originating from the outer-shell atoms of the ring and that when these multiple scattering contributions are included in the analysis, an exact simulation of the raw, unfiltered EXAFS can be obtained. Furthermore, in favorable circumstances, we have been able to show that analysis of the multiple scattering contributions from the outer-shell atoms can help to determine the number of coordinated imidazoles in an unknown structure.

Pyridine is structurally analogous to imidazole as a ligand, and it is to be expected that multiple scattering from the outer-shell carbon atoms of the ring will be important. Table I shows the atom-labeling scheme for the pyridine ring used in the present study, the important double and triple scattering pathways, and the angles involved in these pathways. The intensity of the multiple scattering interaction between three atoms M–X–Y is maximum when the three atoms are collinear and attenuates rapidly as the M–X–Y angle decreases from 180°.[26,29] Thus, for the pyridine ring we expect a strong contribution from C4 (180°) and C3/C5 (150°) and a lesser contribution from C2/C6 (120°).

In the present study we have applied the multiple scattering approach to the analysis of both the crystallographically characterized dicopper(I) complexes **2** and **3′** and the oxygenated complexes **4–6**. In view of the pronounced differences in EXAFS and Fourier transforms between the two sets of data (Figure 2), and in order to increase our confidence in the validity of the multiple scattering treatment for pyridine rings, we have also applied the analysis to other crystallographically characterized copper–pyridine complexes, namely $[Cu^{I}TEPA]BPh_4$[32] (**7**), and the two dinuclear Cu(II) complexes, $[Cu_2N3PY2(OMe)_2](ClO_4)_2$[30] (**8**) and $[Cu_2XYL\text{-}O\text{-}(OH)](PF_6)_2$[31] (**9**) (Scheme I). The Cu K edge EXAFS and Fourier transforms of the dicopper(II) model complexes are also shown in Figure 2, and it can be seen that, like the absorption edges, the data for the oxygenated derivatives resemble these more closely than the dicopper(I) precursor complexes **2** and **3′**. In the following discussion we describe the analysis of each of the structurally characterized model compounds **2**, **3′**, and **7–9** and then use the results of this analysis to draw conclusions regarding the structure of the oxygenated complexes **4–6**.

$[Cu_2N3ORPY2](PF_6)_2$ (2).[21] The coordination of copper in **2** consists of two well-separated three-coordinate moieties, and the X-ray crystal structure is presented in detail elsewhere.[21] The Fourier transform (Figure 2a) consists of three strong peaks assigned (in order of increasing radial distance) to N1, C2/C6, and a composite C3/C4/C5 peak. The EXAFS shows a high-frequency beat pattern at low k, which can be eliminated by Fourier filtering the data from the first two shells only (data not shown) and can thus be assigned to the outermost shell (C3/C4/C5). By analogy to the imidazole case, this high-frequency component is expected to arise almost entirely from multiple scattering. Furthermore, it is present in the EXAFS of all the Cu(I) complexes shown in Figure 2a–c and appears to be a "signature" of Cu(I)–pyridine coordination.

A simulation of the EXAFS and Fourier transform of **2** using the multiple scattering treatment is shown in Figure 3. The simulation successfully reproduces the high-frequency beat pattern, all of the features of both EXAFS and Fourier transform using the distances given in Table II, and the expected angles of 180° (C4), 150° (C3/C5), and 120° (C2/C6) for the multiple scattering pathways. Comparison of these EXAFS-generated distances with their crystallographic counterparts (Table II) indicates close agreement between the two sets of data. However, it is important to note that not all the atoms in the structure contribute to the EXAFS. Thus in addition to the atoms belonging to the

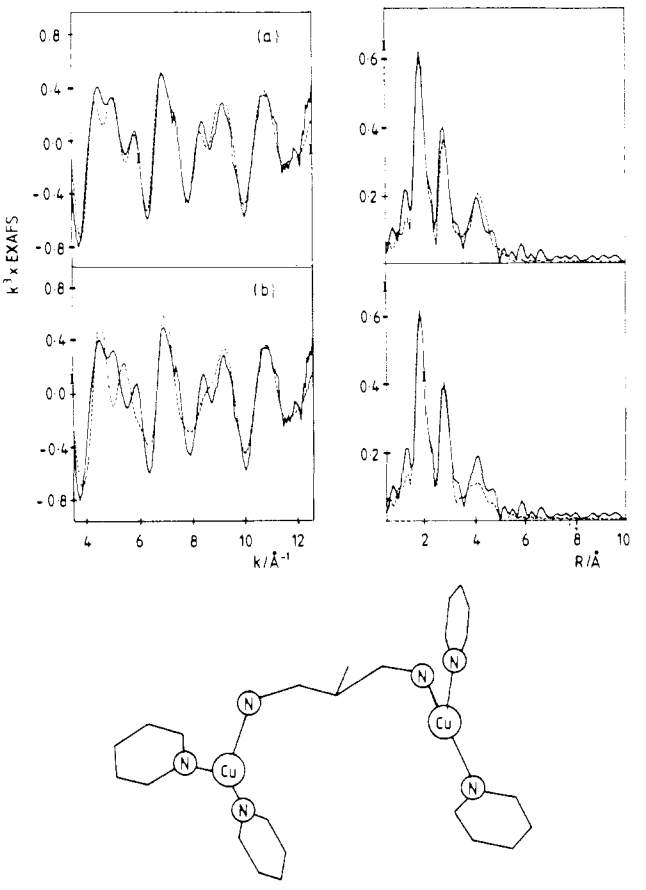

Figure 3. k^3-Weighted experimental (solid line) versus simulated (dotted line) Cu K EXAFS and Fourier transforms for complex **2**: (a) simulation including multiple scattering; (b) simulation using single scattering only.

Table II. Parameters Used To Simulate the Theoretical EXAFS Fits Shown in Figures 3–5[a]

shell	R_{EXAFS}/Å	R_{av}(cryst)/Å	$2\sigma^2$/Å^2
	Complex **2**		
2 N(py)	1.91	1.899	0.003
1 N(amino)	2.20	2.215	0.009
2 C(py)	2.80	2.829	0.008
2 C(py)	2.85	2.860	0.009
2 C(py)	4.14	4.127	0.017
2 C(py)	4.21	4.178	0.017
2 C(py)	4.66	4.638	0.017
	Complex **3′**		
2 N(py)	1.94	1.940	0.006
1 N(amino)	2.14	2.144	0.040
2 C(py)	2.83	2.860	0.007
2 C(py)	2.85	2.886	0.007
2 C(py)	4.18	4.156	0.014
2 C(py)	4.18	4.185	0.014
2 C(py)	4.70	4.680	0.014
1 Cl(ClO_4)	3.38	3.41	0.020
	Complex **7**		
3 N(py)	1.99	2.018	0.007
1 N(amino)	2.24(8)	2.192	0.033
3 C(py)	2.88	2.922	0.007
3 C(py)	2.94	2.951	0.007
3 C(py)	4.22	4.241	0.013
3 C(py)	4.30	4.272	0.013
3 C(py)	4.71	4.785	0.013

[a] The EXAFS distances are compared with the average crystallographic distances (R_{av}(cryst)) for complexes **2**, **3′**, and **7** (Scheme I). Unless otherwise indicated (by parentheses), estimated errors are ±0.03 Å for inner-shell and ±0.05 Å for outer-shell distances.

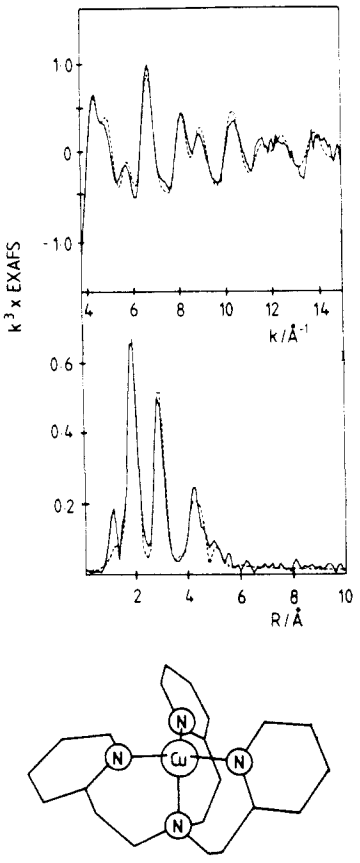

Figure 4. k^3-Weighted experimental (solid line) versus simulated (dotted line) Cu K EXAFS and Fourier transforms for complex **7**.

rigid planar pyridine rings, inclusion of the amino N atom at 2.20 Å improves the fit significantly, but the aliphatic carbon atoms in the structure do not contribute to the EXAFS or Fourier transform. We conclude that the extra rotational and vibrational degrees of freedom available to these aliphatic carbons increase the root-mean-square displacement of their positional coordinate along the absorber–scatterer vector and thus increase the Debye–Waller factor to an extent that renders the atom indetectable. However, low-Z scatterers such as carbon at radial distances up to ca. 4 Å would still be expected to make a small contribution at low energy even if the Debye–Waller term is very large, and we note that in contrast to tetrakis(imidazole)copper(II) complexes,[25] the region below $k = 4$ Å^{-1} is not well fit in the more complex ligand systems described in the present study.

The data in Table II indicate that, like imidazole,[25,28] the pyridine rings can be treated as structural entities that retain their geometry. This means that the first-shell Cu–N distance determines the radial positions of all the other atoms in the rings, so that the number of truly independent variables that need to be refined is reduced greatly. In practice this means that simulations predicting outer-shell distances inconsistent with fixed-ring geometry can be discarded.

The importance of the multiple scattering contribution to the EXAFS spectrum is clearly demonstrated in Figure 3b in which the multiple scattering from the outer shells has been omitted.

[Cu^{I}TEPA](BPh$_4$) (7).[32] The monocation [Cu^{I}TEPA]$^+$ has a trigonal-pyramidal structure with three ligands coordinated in the basal plane (Cu–N = 2.0 Å) and an apical tertiary amino nitrogen ligand at a longer distance (2.2 Å). The k^3-weighted EXAFS and Fourier transform are shown in Figure 4. The simulation has successfully reproduced all the features of the experimental spectrum with the structural parameters given in Table II. Agreement with crystallography is entirely satisfactory, and once again it is evident that the pyridine rings can be refined as structural units that maintain their expected geometry. The amino N atom refines to within 0.02 Å of its crystallographic position, but its Debye–Waller factor (0.035 Å^2) is much larger than that

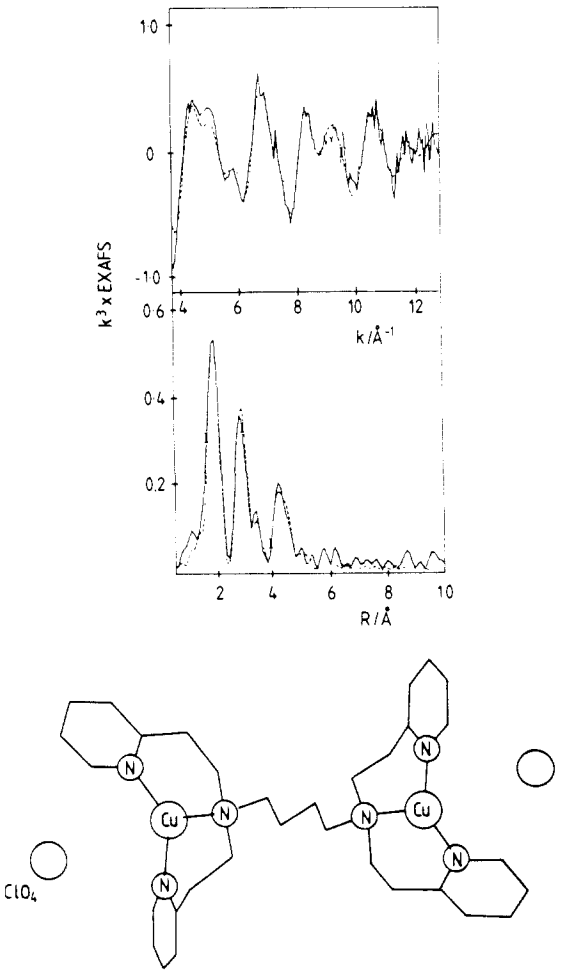

Figure 5. k^3-Weighted experimental (solid line) versus simulated (dotted line) Cu K EXAFS and Fourier transforms for complex **3′**.

found for the amino N atom in **2** (0.009 Å^2), suggesting that the Cu–N(amino) bond is much weaker in the TEPA complex.[34] Again, the aliphatic carbon atoms appear to make no detectable contribution to the EXAFS above $k = 4$ Å^{-1}.

[Cu$_2$N4PY2](ClO$_4$)$_2$ (3′).[20b] The dication **3′** has a similar structure to **2** involving two short pyridine ligands and a longer amino N bonded to the Cu center. However, an important difference is the close approach of the perchlorate counterion to within 2.5 Å of the Cu(I) in the N4PY2 complex. This has the effect of decreasing the PY–Cu–PY angle from 158° in **2** to 139° in **3′** and causes a lengthening of the average crystallographic Cu–N(PY) bond length from 1.90 to 1.94 Å. The structure thus approximates to a highly distorted flattened tetrahedron with the perchlorate anion at the apex.

The k^3-weighted EXAFS and Fourier transform associated with the Cu K edge of **3′** is shown in Figure 5. The simulation accurately reproduces the experimental data, including the high-frequency beats in the low-k region. The pattern of peaks in the Fourier transform is similar to that seen in both [CuTEPA](BPh$_4$) (**7**) and [Cu$_2$N3ORPY2](PF$_6$)$_2$ (**2**), except for the presence of an additional resolved peak of medium intensity around ca. 3.3 Å. In initial simulations we attempted to simulate this feature by a shell of two or three carbon atoms at 3.13 Å, in addition to the four carbon atoms from the pyridine rings found 2.85 Å from the Cu. However, as already stressed, the aliphatic carbon atoms of the ligand do not contribute to the EXAFS of **2** or **7**, and there is no reason why **3′** should behave differently

(34) It should be noted that the Debye–Waller factor for the first-shell Cu–N(py) distance is also larger than that found in **2** measured at comparable temperatures. The observed differences may be due to the increase in coordination number from 3 in **2** to 4 in **7**. A similar effect may explain the ill-defined Cu–N(amino) distance in the pseudotetrahedral **3**.

Table III. Parameters Used To Simulate the Theoretical EXAFS Fits Shown in Figures 6 and 7[a]

shell	R_{EXAFS}/Å	R_{av}(cryst)/Å	$2\sigma^2$/Å^2
	Complex **8**		
2 O(methoxide)	1.93	1.934	0.006
2 N(py)	2.02	1.998	0.006
1 N(amino)	2.33	2.363	0.009
2 C(py)	2.93	2.889	0.007
2 C(py)	2.93	2.994	0.007
Cu–Cu	3.06	3.070	0.009
3 C	3.31		0.006*
2 C(py)	4.25	4.277	0.014
2 C(py)	4.25	4.203	0.014
2 C(py)	4.75		0.014
	Complex **9**		
2 O(OH, phenoxo)	1.93	1.962	0.005
2 N(py, amino)	2.05	2.023	0.005
1 N(py)	2.28	2.204[b]	0.010
2 C(py)	2.89	2.940	0.008
2 C(py)	2.89	3.08[b]	0.008
Cu–Cu	3.06	3.082	0.009
2 C	3.37	*c*	0.006
1 C(py)	4.20	4.255	0.015
1 C(py)	4.20	4.255	0.015
1 C(py)	4.70	4.755	0.015

[a] The EXAFS distances are compared with the average crystallographic distances (R_{av}(cryst)) for complexes **8** and **9** (Scheme I). Unless otherwise indicated (by parentheses), estimated errors are ±0.03 Å for inner-shell and ±0.06 Å for outer-shell distances. [b] The value given is the average distance (over both Cu(II) centers) for the axial pyridine group. A large spread in values (0.20 Å for C2/C6 and 0.35 Å for C3/C5) is found between axial py groups at each Cu(II) center. [c] No carbons from ligated pyridine rings are found at this distance, but a number of carbon atoms from connecting groups, e.g. the bridging phenolate, may contribute here.

in this respect. In later simulations we have found that the peak can be well fit by a chlorine atom from the perchlorate group at 3.37 Å, which is close to its crystallographic position (Table II). In view of the contribution to the EXAFS made by the Cl atom, it is surprising that the O atom from the perchlorate group at 2.5 Å does not appear to contribute.

The correspondence between EXAFS and crystallographic distances is shown in Table II. The agreement for Cu–pyridine distances is again excellent. However, the Cu–N(amino) interaction is not well-defined, and acceptable fits have been obtained with Cu–N(amino) distances between 2.03 and 2.13 Å. The Debye–Waller term is high, and we must conclude that the Cu–N(amino) linkage is again rather weak.[34]

Dinuclear Copper(II) Complexes and Cu–Cu Distances. The dicopper(II) compounds $[Cu_2N3PY2(OMe)_2](ClO_4)_2$ (**8**) and $[Cu_2(XYL\text{-}O\text{-})OH](PF_6)_2$ (**9**) have five-coordinate square-pyramidal structures with two bridging groups connecting the Cu(II) centers (Cu–Cu = 3.07 and 3.08 Å, respectively).[17a,30,31] Both complexes are formed as the result of aerial oxidation of three coordinate Cu(I) complexes; thus, **8** is formed when **1** is allowed to react with dioxygen in methanol at room temperature,[30] whereas **9** is formed by a similar reaction of the related *m*-XYL-bridged dicopper(I) complex in dichloromethane.[31] In **8**, the two pyridine ligands and two methoxy groups form the equatorial plane (Cu–N(py) = 2.0 Å) and the amino N atom occupies an axial position (Cu–N(amino) = 2.3 Å); in **9**, one pyridine is equatorial while the other now occupies the axial position. Thus, differences in the multiple scattering from the pyridine outer-shell carbons would be expected in the two complexes.

It is evident from the spectra shown in Figure 2 that the EXAFS and Fourier transforms for the dicopper(II) models **8** and **9** resemble those of the oxygenated complexes and differ from those of the Cu(I) precursors in two important respects: (i) The characteristic high-frequency beat pattern is absent in the low-energy region of the EXAFS. (ii) The amplitude of the outermost peak in the transform has been reduced, especially in compound **9**. Good simulations of spectra for both complexes have been obtained and are shown in Figures 6 and 7 with the associated

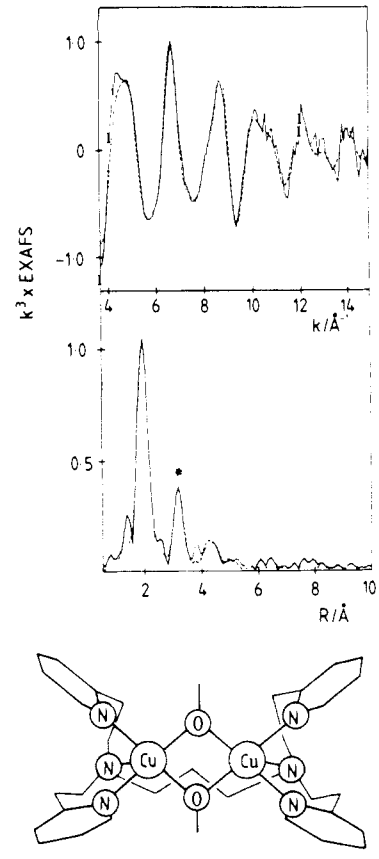

Figure 6. k^3-Weighted experimental (solid line) versus simulated (dotted line) Cu K EXAFS and Fourier transforms for complex **8**.

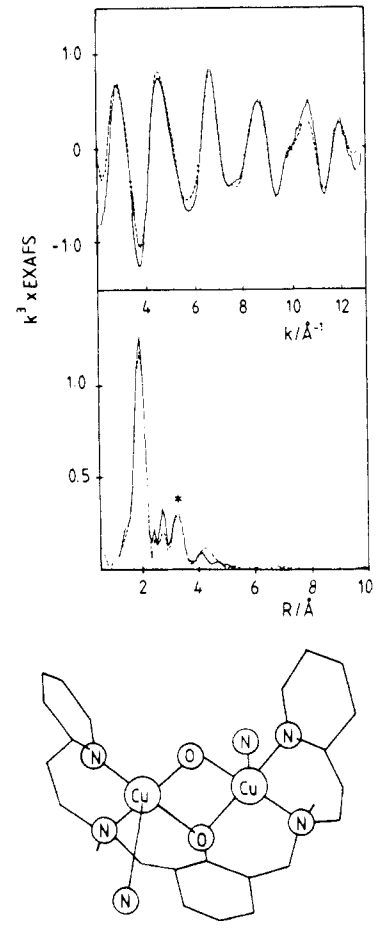

Figure 7. k^3-Weighted experimental (solid line) versus simulated (dotted line) Cu K EXAFS and Fourier transforms for complex **9**.

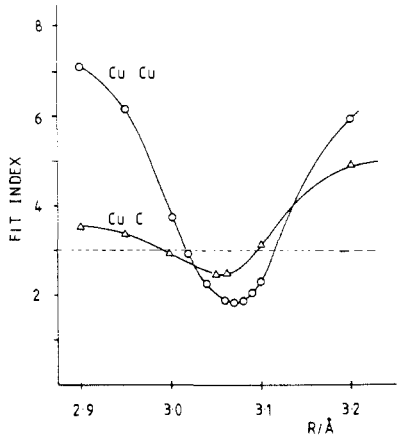

Figure 8. Cu–Cu versus Cu–C assignment of outer-shell peaks for complex **8**. Least-squares fitting index (k^3 weighted) plotted as a function of Cu–Cu distance or Cu–C distance in the range 2.9–3.2 Å. Dotted line represents the value of the fit index with no scatterer at that distance. For further details see the text.

structural parameters given in Table III. Whereas **8** has been fitted by including multiple scattering from two pyridine groups at 2.0 Å, **9** could only be fitted using multiple scattering from a *single* pyridine group at this distance. The longer (axial) pyridine group at ca. 2.25 Å does not appear to contribute significantly to either the EXAFS or Fourier transform in the R = 4–5 Å region. One factor contributing to the absence of outer-shell intensity from the axial pyridine is the increased distance of the C3/C4/C5 group of carbons from the copper (Cu–C4 = 5.0 Å in **9** as opposed to 4.75 Å for equatorial py in **8** and 4.65 Å for Cu–C4(py) in **2**). In addition, whereas **8** contains a crystallographic twofold axis bisecting the Cu–Cu vector such that each Cu(II) center has identical coordination, the two Cu(II) centers in **9** are crystallographically inequivalent,[30,31] leading to a "smearing out" of the outer-shell intensity (i.e., large Debye–Waller term). Similar effects have been observed in other dicopper(II) complexes of the XYL-O- ligand system,[35] all of which contain one axial and one equatorial pyridine group.[36] Thus, although the reason for the lack of outer-shell intensity is incompletely understood, it may be a useful indicator of the presence of axial pyridine in the five-coordinate dicopper(II) complexes.

Copper–Copper Distances. The X-ray absorption edge data of Figure 1 have established that the oxidation state of the oxygenated compounds **4–6** is +2. The observed dioxygen binding stoichiometry of 1:2 O_2 to Cu, together with the total absence of an EPR spectrum,[20] would then suggest peroxide coordination within a coupled binuclear Cu(II) site. It is important to know the Cu–Cu separation when attempting to elucidate the mode of peroxide coordination from physical techniques including EXAFS. Thus, we have recently reported[19] that a Cu(II)–peroxo complex of the related XYL-O- ligand system exhibits a Cu–Cu distance of 3.31 ± 0.04 Å, and the determination of this distance in conjunction with a normal-coordinate analysis of the resonance Raman spectrum[18] has led to the proposal of an asymmetric μ-1,2-bridged or terminally coordinated structure for peroxide in the $[Cu_2(XYL\text{-}O\text{-})(O_2)]^+$ monocation. However, our experience with the latter system has shown that the Cu–Cu interaction is not always easy to separate from the contribution from outer-shell carbon atoms of the pyridine rings. Careful analysis of the outer-shell peaks in the Fourier transforms of structurally characterized dinuclear Cu(II) complexes of the same or closely related ligand systems is most useful in identifying the presence (or absence) of a Cu–Cu wave.

(35) Blackburn, N. J.; Strange, R. W.; Karlin, K. D.; Farooq, A., manuscript in preparation.
(36) (a) Karlin, K. D.; Hayes, J. D.; Hutchinson, J. P.; Zubieta, J. *J. Chem. Soc., Chem. Commun.* **1983**, 376–378. (b) Karlin, K. D.; Cohen, B. I.; Hayes, J. C.; Farooq, A.; Zubieta, J. *Inorg. Chem.* **1987**, *26*, 147–153. (c) Karlin, K. D.; Farooq, A.; Hayes, J. C.; Cohen, B. I.; Zubieta, J. *Inorg. Chem.* **1987**, *26*, 1271–1280.

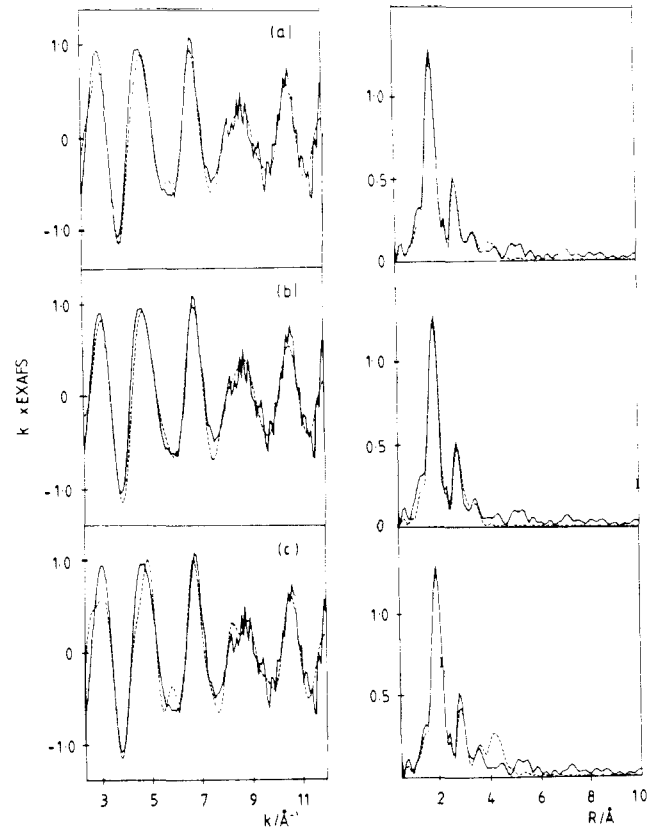

Figure 9. k^3-Weighted experimental (solid line) versus simulated (dotted line) Cu K EXAFS and Fourier transforms for the oxygenated complex **6**. The analysis was carried out using multiple scattering contributions from (a) a single pyridine group, (b) zero pyridine groups (i.e., single scattering only), and (c) two pyridine groups.

The Cu–Cu distances (indicated in the Fourier transforms in Figures 6 and 7 by asterisks) refine to 3.06 Å in both **8** and **9**. We have carried out a detailed analysis of the uniqueness of the assignment of the Cu–Cu interactions by computing the least-squares fit index as a function of scatterer distance for (i) a single copper and (ii) two additional carbons at this distance, all other variable parameters being kept fixed at the values listed in Table III. The calculation utilized the complete range of unfiltered k^3-weighted EXAFS data and included the multiple scattering contribution from the outer shells of the pyridine rings. The results are shown for complex **8** in Figure 8. In the case of Cu as the scatterer, a deep minimum is observed, equivalent to an improvement in fit index of 70% over no scatterer at the same distance, but in the case of carbon, a shallow minimum with only a 20% improvement is observed. Complex **9** gives similar results. In neither case do the carbon fits reproduce the beat patterns for k = 10–13 Å^{-1}, which arise as the result of the copper wave having maximum amplitude in this region.[19] Thus, the Cu–Cu waves in the dicopper(II) model compounds are well-defined, and the Cu–Cu distances can be determined with some confidence.

Oxygenated Complex $[Cu_2(N4PY2)(O_2)]^{2+}$ (6). The experimental data for complex **6** were of better quality than that of **4** or **5** and were therefore chosen for detailed analysis. Figure 9a shows the best simulation of the k^3-weighted EXAFS and Fourier transform, and the structural parameters associated with this simulation are given in Table IV. The Cu(II) appears to be coordinated to four first-row scatterers (O and N) at 1.97 Å. Inclusion of a low-Z scatterer at 2.56 Å (as a fifth ligand to copper) results in a small decrease in the value of the fit index (from 2.45 to 2.31) and a visible improvement in quality of fit in the region k = 5.5–6.5 Å^{-1}. Analysis of outer-shell contributions indicates a shell of four carbons at 2.86 Å (consistent with C2/C6 atoms of pyridine rings) and a shoulder in the transform (marked by an asterisk) corresponding to a Cu–Cu distance of 3.37 ± 0.04 Å. The Cu–Cu interaction is not as well-defined as in **8** or **9**, but

Table IV. Parameters Used To Simulate the Theoretical EXAFS Fits of the Oxygenated Complexes **4**–**6** Shown in Figures 9, 11, and 12[a]

shell	R_{EXAFS}/Å	$2\sigma^2$/Å^2
	Complex **6**	
4 N or O	1.97	0.006
1 N	2.56	0.004
2 C(py)	2.86	0.007
2 C(py)	2.86	0.007
Cu–Cu	3.37	0.017
1 C(py)	4.25	0.017
1 C(py)	4.25	0.017
1 C(py)	4.70	0.017
	Complex **4**	
4 N or O	1.99	0.006
2 C	2.90	0.010
2 C	2.90	0.010
Cu–Cu	3.22	0.022
	Complex **5**	
4 N or O	1.97	0.007
2 C	2.82	0.010
2 C	2.94	0.010
Cu–Cu	3.31	0.034

[a] Unless otherwise indicated (by parentheses), estimated errors are ±0.03 Å for inner-shell and ±0.06 Å for outer-shell distances.

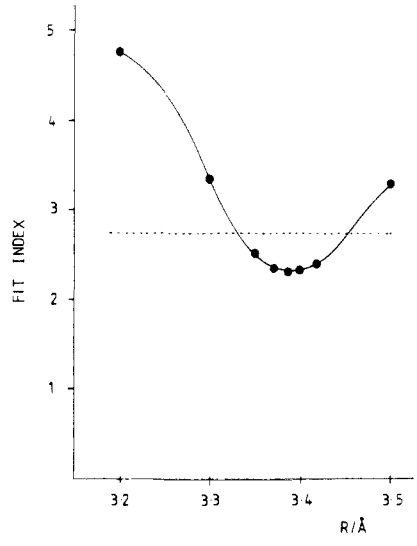

Figure 10. Determination of Cu–Cu distance in the oxygenated complex **6**. Effect of including a Cu scatterer in the fit. Least-squares fit index (k^3 weighted) plotted as a function of Cu–Cu distance. The dotted line represents the value of the fix index with no scatterer at that distance.

a plot of fit index versus Cu···Cu separation shows a respectable minimum with a 15% improvement in fit index relative to no scatterer at this distance; on the other hand, the analysis with two additional carbons replacing the Cu–Cu wave gives no least-squares minimum. These results are shown in Figure 10. Thus, although the assignment of the Cu–Cu interaction must be made with caution, the value of 3.38 Å is not inconsistent with other experimental data on this[20] and related systems,[19] including the O_2 binding stoichiometry of 2:1 Cu to O_2 and the absence of an EPR spectrum.

An important aspect of the Fourier transform of **6** is the almost negligible intensity of the outer-shell peaks attributable to C3/C4/C5 atoms of the pyridine rings. As in the case of **9**, the simulation shown in Figure 9a has included multiple scattering from the outer-shell C3/C4/C5 carbons of a single pyridine group (Cu–N(py) = 1.97 Å). Parts b and c of Figure 9 show simulations involving multiple scattering from zero and two pyridines, respectively. The simulation involving two pyridines is clearly unsatisfactory. Two explanations of these data would seem possible. The structure of the oxygenated complex **6** may involve only a single equatorially coordinated pyridine, analogous to the

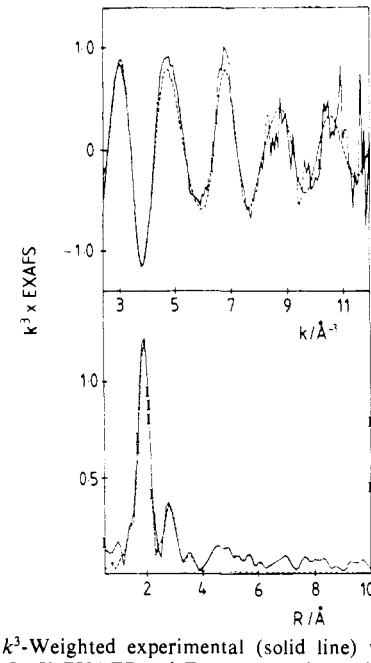

Figure 11. k^3-Weighted experimental (solid line) versus simulated (dotted line) Cu K EXAFS and Fourier transforms for complex **4**.

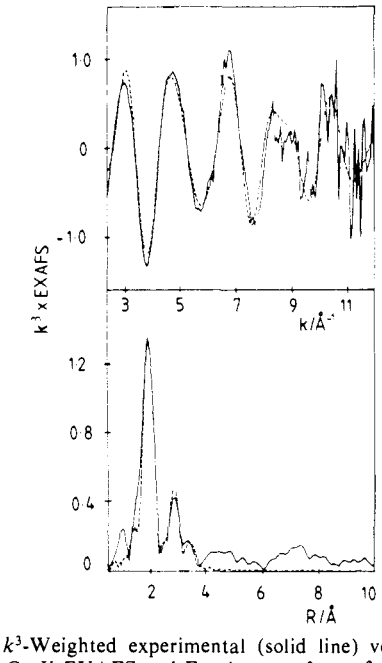

Figure 12. k^3-Weighted experimental (solid line) versus simulated (dotted line) Cu K EXAFS and Fourier transforms for complex **5**.

structures of **9** and related systems,[36] with the second pyridine occupying an axial position. Alternatively, the lack of multiple scattering could arise if the pyridine coordination was disordered as the result of structural inequivalence of individual Cu(II) centers of the dinuclear pair.

Oxygenated Complexes $[Cu_2(N3PY2)(O_2)]^{2+}$ (4) and $[Cu_2(N3ORPY2)(O_2)]^{2+}$ (5). The EXAFS data for **4** and **5** resemble that of **6** except that they are of generally poorer quality. Simulations have been obtained and are shown in Figures 11 and 12 and Table IV. The structural parameters are similar to those found for **6**, with weak Cu–Cu interactions and tentative Cu–Cu distances of 3.25 and 3.32 Å, respectively. Adequate fits to the raw data can be obtained without inclusion of any multiple scattering interactions, suggesting either axial–equatorial, disordered pyridine coordination, or both.

Conclusions

The analysis presented in this study allows us to draw certain conclusions concerning the mode of binding of dioxygen to copper

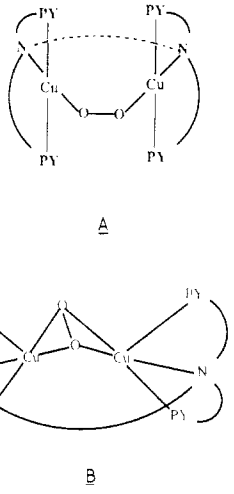

A

B

Figure 13. Suggested structures for the oxygenated complexes of the NnPY2 and N3ORPY2 ligand systems.

in the N3PY2, N3ORPY2, and N4PY2 systems. The stoichiometry of dioxygen binding to the dicopper(I) precursors $[Cu_2(L)]^{2+}$ (Cu:O = 2:1) allows for the formulation of these complexes as $[Cu_2(L)(O_2)]^{2+}$ species. The X-ray absorption edge data have allowed the assignment of the oxidation state in these compounds as Cu(II), and confirmatory spectroscopic evidence comes from the observation of d–d bands in these complexes [e.g., λ_{max} = 775 nm (ϵ = 200 M^{-1} cm^{-1}) for $[Cu_2(L)(O_2)]^{2+}$ (**6**)], which would be lacking in a d^{10} Cu(I)-containing complex.[20] We can predict with some confidence that the reduced dioxygen species O_2^{2-} bridges the two Cu(II) atoms on the basis of the observed Cu–Cu wave found in $[Cu_2(L)(O_2)]^{2+}$. The presence of a bridging ligand is also supported by the lack of an observable EPR spectrum for **6**, and solutions (−80 °C) of this dioxygen complex also exhibit ^1H NMR spectra essentially unchanged from those of the precursor complexes $[Cu_2(L)]^{2+}$, suggesting that strong magnetic coupling of the Cu(II) ions is effected.[20] The EXAFS analysis has provided evidence for four oxygen or nitrogen donors at 1.97 Å, with some suggestion of a fifth ligand at a longer distance (2.58 Å). When combined with the magnitude of the Cu–Cu distance (3.37 Å), this puts limits on the possible bridging modes of the putative peroxide ligand.

The likely modes of binding of a peroxo ligand to a dicopper(II) center in **6** are a μ-1,2 bridge or a μ-1,1 bridge. As discussed above, the μ-1,2-peroxo coordination to Cu(II) is proposed for oxyhemocyanin,[3] and both *cis*- and *trans*-μ-1,2-superoxo- and -peroxodicobalt compounds are well established.[37] A μ-1,1-peroxo bridging mode has been considered and ruled out for oxyhemocyanin[38] and oxyhemerythrin,[39] but such an entity has been proposed in cobalt systems.[40]

The trans planar μ-1,2-peroxo coordination can be ruled out here because it requires a Cu···Cu distance of greater than 4 Å,[37] but as the μ-1,2 linkage is distorted from planarity, the M···M distance shortens and a distance as low as 3.1 Å has been reported in a peroxodicobalt(III) complex.[41] On the basis of present EXAFS analysis and on model-building studies, we present two possible structures for compounds **4**–**6** for consideration. In structure A (Figure 13) a 3.37-Å Cu···Cu distance predicts reasonable hybridization at the coordinated oxygen atoms,[37] and when a model of the structure is built, it can be seen that a stacked configuration for the pyridine rings of adjacent tridentate units of the N4PY2 ligand would ensue. Such stacking has indeed been observed in a structurally characterized bridged dicopper(II) complex of a similar ligand.[42] In structure A, the inner coordination sphere would consist of the three nitrogen donors of the tridentate ligand plus one oxygen donor from the coordinated peroxo group. However, neither the 2.5-Å distance (Table IV) nor the evidence for one axially coordinated pyridine group per Cu(II) can be accommodated within this structure.[43] Structure B (Figure 13) may be thought of as a symmetrically bridged η^2:η^2 species. Here, the inner coordination shell would consist of two nitrogen donors and two peroxo oxygen atoms. A third nitrogen donor (py) at a longer distance (2.56 Å) is consistent with both the EXAFS data and the tendency of planar four-coordinate Cu(II) to achieve pentacoordination as exemplified by the structure of compound **8**[30] and others.[32,36,42] Side-on coordination is not unknown in peroxometal complexes,[37,44-47] and a structurally analogous dicopper(I)–acetylene complex has been reported recently.[48] The observed Cu···Cu distance of 3.37 Å in **6** would require a nonplanar $Cu_2(O_2)$ unit, which is also observed in the dicopper–acetylene structure described.[48]

For compounds **4** and **5** the Cu···Cu distance is determined with less confidence. However, the details of the EXAFS analysis appear similar to that for **6**, and similar structures would appear likely.

Thus, dicopper complexes of the dinucleating ligands L mimic to a significant extent a number of properties of hemocyanins, including the reversible binding of CO and O_2 and major features of the UV–vis spectrum. The X-ray absorption studies described here confirm that the dioxygen adducts $[Cu_2(L)(O_2)]^{2+}$ are Cu(II)-containing species. Along with other spectroscopic evidence (e.g., UV–vis, EPR, NMR),[20] the Cu–Cu distances observed (3.2–3.4 Å) by EXAFS spectroscopy suggest that a peroxo (O_2^{2-}) ligand bridges and magnetically couples the two Cu(II) ions in $[Cu_2(L)(O_2)]^{2+}$; the detailed EXAFS analysis leads us to suggest two possible structures for these dioxygen (peroxo) complexes, including an η^2:η^2 structure, not previously considered in copper/O_2 chemistry. The similarity of chemical and spectral properties of $[Cu_2(L)(O_2)]^{2+}$ with oxyhemocyanin could lead one to speculate that an "endogenous" bridging ligand is not required to account for the observed UV–vis features and the EPR silence and strong magnetic coupling found in the protein dioxygen carrier; this would be in accord with the recent crystal structure of deoxy-Hc.[6] However, since the presence of a band at 420 nm in oxy-Hc and analogies of oxy-Hc properties to certain met-Hc forms provide good evidence for the presence of an additional bridging ligand other than peroxo,[3] the presence of a OH^- or H_2O bridging ligand is not precluded.

Note Added in Proof. We have recently reported the first X-ray structure of a copper–dioxygen complex of a related ligand system: Jacobson, R. R.; Tyeklar, Z.; Farooq, A.; Karlin, K. D.; Liu, S.; Zubieta, J. *J. Am. Chem. Soc.*, in press.

Acknowledgment. We gratefully acknowledge financial support from the Science and Engineering Research Council of the U.K. to N.J.B. and the National Institutes of Health to K.D.K. We

(37) Gubelman, M. H.; Williams, A. F. *Struct. Bonding (Berlin)* **1983**, *55*, 1–65.
(38) Thamann, T. J.; Loehr, J. S.; Loehr, T. M. *J. Am. Chem. Soc.* **1977**, *99*, 4187.
(39) Kurtz, D. M.; Shriver, D. F.; Klotz, I. M. *J. Am. Chem. Soc.* **1976**, *98*, 5033.
(40) Burgand, R. R., Jr.; Bencosme, C. S.; Collman, J. P.; Anson, F. C. *J. Am. Chem. Soc.* **1983**, *105*, 2710–2718.
(41) Suzuki, M.; Ueda, I.; Kanatomi, H.; Murase, I. *Chem. Lett.* **1983**, 185–188.
(42) Karlin, K. D.; Gultneh, Y.; Hayes, J. C.; Zubieta, J. *Inorg. Chem.* **1984**, *23*, 519–521.
(43) In complexes $[Cu_2(L)(O_2)]^{2+}$, the EXAFS analysis suggests that μ-1,1-peroxo coordination is a less likely structural possibility for the same reason as the μ-1,2 structure; it is also considered unlikely since there is no coordination chemistry preference for it in a nonprotonated form.[37-40]
(44) Boeyens, J. C. A.; Haegele, R. *J. Chem. Soc., Dalton Trans.* **1977**, 648–650.
(45) Bradley, D. C.; Ghota, J. S.; Hart, F. A.; Hursthouse, M. B.; Raithby, P. R. *J. Chem. Soc., Dalton Trans.* **1977**, 1166–1172.
(46) Bennett, M. J.; Donaldson, P. B. *Inorg. Chem.* **1977**, *16*, 1585–1589.
(47) (a) Sakurai, F.; Suzuki, H.; Moro-oko, Y.; Ikawa, T. *J. Am. Chem. Soc.* **1979**, *102*, 1749–1751. (b) Sugimoto, R.; Eikawa, H.; Suzuki, H.; Moro-oko, Y.; Ikawa, T. *Bull. Chem. Soc. Jpn.* **1981**, *54*, 2849–2850.
(48) Villacorta, G. M.; Gibson, D.; Williams, I. D.; Lippard, S. J. *J. Am. Chem. Soc.* **1985**, *107*, 6732–6734.

thank the Daresbury Laboratory for use of facilities and provision of beam time. We also thank the NATO Scientific Affairs Bureau for the award of a travel grant (RG.82/0139) to N.J.B. and K.D.K.

Registry No. 1, 114301-10-9; 2, 114301-13-2; 3, 112022-71-6; 3', 114301-11-0; 4, 98218-48-5; 5, 114301-14-3; 6, 112022-74-9; 7, 82384-51-8; 8, 88920-97-2; 9, 86593-50-2; N3PY2, 88917-40-2; N3ORPY2, 114301-08-5; N4PY2, 98218-51-0.

Supplementary Material Available: Tables 5-12 of raw (background-subtracted) EXAFS data for compounds **2**, **3'**, **7**, **8**, **9**, **6**, **4**, and **5** respectively (70 pages). Ordering information is given on any current masthead page.

Metal Complexes with Tetrapyrrole Ligands. 50.[1] Redox Potentials of Sandwichlike Metal Bis(octaethylporphyrinates) and Their Correlation with Ring-Ring Distances

Johann W. Buchler* and Bernd Scharbert

Contribution from the Institut für Anorganische Chemie, Technische Hochschule Darmstadt, D-6100 Darmstadt, Germany. *Received October 13, 1987*

Abstract: On the basis of prior work describing the synthesis and structure of sandwichlike metal bis(porphyrinates) $M(OEP)_2$ (**1**; M = Y, La, ..., Lu, except Pm), the electron-transfer reactions of these double-deckers are presented. Apart from the Ce^{IV} complex $Ce(OEP)_2$ (**1c**), all the other species contain M^{III} ions that are not affected in the redox reactions. The neutral M^{III} complexes **1** are porphyrin π-radicals yielding the porphyrin π-diradical cations $[M(OEP)_2]^+$ (**2**) upon reversible one-electron oxidation and the monoanions $[M(OEP)_2]^-$ (**3**) or the porphyrin π-radical dianions $[M(OEP)_2]^{2-}$ (**4**) upon reversible one- or two-electron reduction. $Ce(OEP)_2$ (**1c**) is reversibly oxidized to the porphyrin π-radical cation $[Ce(OEP)_2]^+$ (**2c**). The quasi-reversible reduction of **1c** gives the anion $[Ce(OEP)_2]^-$ (**3c**) with Ce^{III}. For the neutral M^{III} complexes **1**, the energies of the near-infrared absorption bands and the redox potentials for the processes **1** $\rightleftarrows$ **2** are correlated with the ionic radii r_i of the tervalent central ions M^{III}. A decrease of the ring oxidation potentials parallels a decrease of the ionic radii and, hence, the ring-ring distances in the double-deckers.

A bacteriochlorophyll *b* dimer $[Mg(Bchl)]_2$,[2] the "special pair", represents the reaction center of bacterial photosynthesis. It is embedded in an extended membrane protein complex and, according to present knowledge, is oxidized by absorption of light quanta according eq 1, which causes the primary charge separation.[3]

$$[Mg(Bchl)]_2 \overset{+e^-}{\rightleftharpoons} [Mg(Bchl)]_2^+ \qquad (1)$$

In the special pair, two tetrapyrrole ligands interact via a $\pi-\pi$ overlap between two pyrrole rings, one of each macrocycle,[4] at a distance of about 300 pm.[3]

Recently, we prepared the sandwichlike metal octaethylporphyrinates $M(OEP)_2$ (**1a-p**; see Table I)[5-10] including yttrium, lanthanum, and all metals of the lanthanoid series except promethium, following our previous work on the similar tetra-*p*-tolylporphyrin double-deckers $M(TTP)_2$ (M = Ce, Pr, Nd).[11,12] Suslick and co-workers recently obtained the actinide derivatives $Th(TPP)_2$ and $U(TPP)_2$.[13]

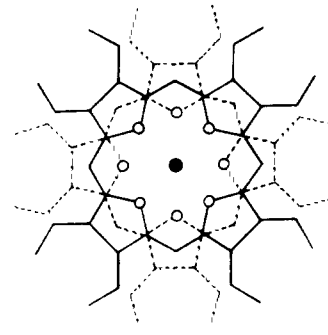

● = M (metal); ○ = N (nitrogen)
$[M(OEP)_2]^n$: **1**, $n = 0$; **2**, $n = 1+$; **3**, $n = 1-$; **4**, $n = 2-$. For specification of metals, see Table I.

The idea has been expressed that these double-deckers show analogies to the special pair in regard to structure and electron configuration.[8,12,14] The structural analogy lies in the face-to-face arrangement of two tetrapyrrole macrocycles. This causes the electronic analogy seen in the following observations: (1) The abstraction of an electron from the porphyrin π-orbitals is easier

(1) Paper 49. Botulinski, A.; Buchler, J. W.; Lee, Y. J.; Scheidt, W. R.; Wicholas, M. *Inorg. Chem.* **1988**, *27*, 927-933.

(2) Abbreviations used: BChl, bacteriochlorophyll *b*; M, metal; $(P)^{2-}$, $(OEP)^{2-}$, $(Pc)^{2-}$, $(TPP)^{2-}$, $(TTP)^{2-}$, $(TClP)^{2-}$, and $(TAP)^{2-}$ are dianions of a general porphyrin, 2,3,7,8,12,13,17,18-octaethylporphyrin, phthalocyanine, 5,10,15,20-tetraphenylporphyrin, 5,10,15,20-tetra-*p*-tolylporphyrin, 5,10,15,20-tetrakis(*p*-chlorophenyl)porphyrin, and 5,10,15,20-tetra-*p*-anisylporphyrin, respectively; Ln, lanthanoid metal; DMF, dimethylformamide; H(acac), acetylacetone; near-IR, near-infrared; SCE, saturated calomel electrode; THF, tetrahydrofuran.

(3) (a) Deisenhofer, J.; Epp, O.; Miki, K.; Huber, R.; Michel, H. *Nature (London)* **1985**, *318*, 618-624. (b) Deisenhofer, J.; Epp, O.; Miki, K.; Huber, R.; Michel, H. *J. Mol. Biol.* **1984**, *180*, 385-398.

(4) Plato, M.; Tränkle, E.; Lubitz, W.; Lendzian, F.; Möbius, K. *Chem. Phys.* **1986**, *107*, 185-196, and references cited therein.

(5) Buchler, J. W.; De Cian, A.; Fischer, J.; Kihn-Botulinski, M.; Paulus, H.; Weiss, R. *J. Am. Chem. Soc.* **1986**, *108*, 3652-3659.

(6) Buchler, J. W.; De Cian, A.; Fischer, J.; Kihn-Botulinski, M.; Weiss, R. *Inorg. Chem.* **1988**, *27*, 339-345.

(7) Buchler, J. W.; Knoff, M. In *Optical Properties and Structure of Tetrapyrroles*; Blauer, G., Sund, H., Eds.; de Gruyter: Berlin, 1985; pp 91-105.

(8) (a) Buchler, J. W.; Elsässer, K.; Kihn-Botulinski, M.; Scharbert, B. *Angew. Chem.* **1986**, *98*, 257-258; *Angew. Chem., Int. Ed. Engl.* **1986**, *25*, 286-287. (b) Scharbert, B. Doctoral Dissertation, Technische Hochschule Darmstadt, 1988.

(9) Buchler, J. W.; Hüttermann, J.; Löffler, J. *Bull. Chem. Soc. Jpn.* **1988**, *61*, 71-77.

(10) (a) Buchler, J. W.; Kihn-Botulinski, M., to be submitted for publication. (b) Kihn-Botulinski, M. Doctoral Dissertation, Technische Hochschule Darmstadt, 1986.

(11) Buchler, J. W.; Kapellmann, H. G.; Knoff, M.; Lay, K. L.; Pfeifer, S. *Z. Naturforsch., B: Anorg. Chem., Org. Chem.* **1983**, *38B*, 1339-1345.

(12) Buchler, J. W.; Elsässer, K.; Kihn-Botulinski, M.; Scharbert, B.; Tansil, S. *ACS Symp. Ser.* **1986**, *321*, 94-104.

(13) Girolami, G. S.; Milam, S. N.; Suslick, K. N. *Inorg. Chem.* **1987**, *26*, 343-344.

(14) Buchler, J. W. *Comments Inorg. Chem.* **1987**, *6*, 175-191.

0002-7863/88/1510-4272$01.50/0